Filling in sewage sludge biodrying gaps: Greenhouse gases, volatile organic compounds and odour emissions

Daniel González [a, b], Nagore Guerra [c], Joan Colón [c], David Gabriel [b], Sergio Ponsá [c], Antoni Sánchez [a, *]

[a] *Composting Research Group (GICOM) Dept. of Chemical, Biological and Environmental Engineering, Universitat Autònoma de Barcelona, 08193-Bellaterra (Barcelona), Spain.*

[b] *Group of biological treatment of liquid and gaseous effluents (GENOCOV) Dept. of Chemical, Biological and Environmental Engineering, Universitat Autònoma de Barcelona, 08193-Bellaterra (Barcelona), Spain*

[c] *BETA Technology Centre: "U Science Tech", University of Vic-Central University of Catalonia, 08500 Vic, Barcelona, Spain*

* Corresponding author:

Antoni Sánchez

Composting Research Group (GICOM), Dept. of Chemical, Biological and Environmental Engineering

Universitat Autònoma de Barcelona

Bellaterra, 08193 (Spain)

Email address: antoni.sanchez@uab.cat

Abstract

In the present work, a complete study of the sewage sludge (SS) biodrying technology was conducted at bench-scale, aiming at assessing its performance and providing a valuable insight into the different gaseous emission patterns found for greenhouse gases (GHG) and odorant pollutants. As process key parameters, temperature, specific airflow, dynamic respiration index, final moisture content and Lower Calorific Value (LCV) were evaluated. At the end of the biodrying, a product with a 35.9% moisture content and a LCV of 7.1 $MJ \cdot kg^{-1}$product was obtained. GHGs emission factor was 28.22 $kgCO_{2eq}$ per Mg of initial mass of dry matter in the SS (DM_0-SS). During the biodrying process, maximum odour concentration measured was 3043 $ou \cdot m^{-3}$ and the estimated odour emission factor of the biological treatment was 3.10E+07 ou per Mg DM_0-SS. Finally, VOCs were completely identified and quantified. The most abundant VOCs found in the biodrying gaseous emissions were terpenes, sulphur-compounds and ketones.

Keywords: Sewage sludge, biodrying, gaseous emission, greenhouse gases (GHG), odour.

1. Introduction

The large amount of sewage sludge (SS) production is becoming a worldwide environmental problem. Nowadays, different treatment processes are used to manage SS produced, such as land application, thermal processing, composting or anaerobic digestion, aiming at reducing its volume and quantity as well as stabilizing it. In fact, composting, which is one of the most applied SS stabilization approaches, is considered as an environmental friendly technology. Nevertheless, there are some limitations when applying SS or the compost obtained from SS on soil due to the possible presence of heavy metals or other emergent contaminants (European Commission, 2014). Regarding that, and taking into account the limited land resources, thermal processes have risen as an attractive sludge treatment option in many countries. However, due to the high water content present in SS, a pre-drying step is required prior to incineration. Between the existing alternatives for SS drying, biodrying is catching attention of researchers in the last years (Huiliñir and Villegas, 2015; Villegas and Huiliñir, 2014; Zhao et al., 2011). The objective of SS biodrying process, which is based on the mechanisms of a composting process, is to remove water from biowaste with high moisture content and to reduce the volume and the biological activity of the solid matrix to obtain a product with a considerable Lower Calorific Value (LCV) and low moisture content that can be used as a biomass fuel (Adani et al., 2002). To this aim, both the metabolic heat generated during the aerobic degradation of the easily biodegradable organic matter as well as forced aeration are used (Frei et al., 2004). In this sense, and compared with composting, higher aeration rates are used during biodrying to enhance water removal (Cai et al., 2013; Yuan et al., 2016).

Different studies have been conducted to find operating strategies to optimize the SS biodrying process in terms of aeration and initial moisture content, as they are the key

parameters to achieve an optimum SS biodrying performance. For example, Cai et al. (2013) studied the influence of aeration on water removal reporting higher evaporation rates at higher aeration rates during the thermophilic phase of the SS biodrying process. Moreover, Huiliñir and Villegas (2015) worked on the simultaneous effect of the aeration and the initial moisture of the material on the water evaporation. They reported that higher material temperature is achieved when initial moisture content is around 68% and that, under these conditions, higher aeration rates enhance water evaporation. However, critical aspects such as gaseous emissions and its associated environmental impacts have not been systematically studied yet as it has been done with SS composting. Greenhouse gases (GHG) and odorant compounds characterization have been widely reported for SS composting at bench-scale (Maulini-Duran et al., 2013; Rincón et al., 2019), whereas few studies have been conducted in full-scale facilities (González et al., 2019a; Shen et al., 2012). Nonetheless, few information about gaseous emissions from bench-scale SS biodrying can be found in literature (Kim et al., 2018; Wei et al., 2016), but with no concluding or profitable information in terms of environmental impact of the technology. In this sense, gaseous emissions assessment studies must be carried out to fill existing knowledge gaps and to help improving the performance of such biological treatment technology. Emission factors referred to specific pollutants are a useful tool for environmental impact assessment and facilitate the estimation of the overall emission rate of a treatment process based on a specific activity index, which should represent the process evaluated (Capelli et al., 2009). The US Environmental Protection Agency defined the emission factor of a specific pollutant as the relation between the quantity of the pollutant emitted to the atmosphere with an activity associated with the release of the pollutant, such as the mass of waste to be treated, the emitting surface or time units (United States Environmental Protection

Agency (USEPA), 1995). Analogously, in the last years this tool has been referenced for the assessment of odour impact from different treatment processes and facilities, namely Odour Emission Factor (OEF) (Capelli et al., 2014; Sironi et al., 2006).

To the authors' knowledge, this is the first bench-scale work where a systematic study of the gaseous emissions generated during the biodrying process of conventional SS is conducted. Due to the lack of this scientific information and its importance for further development of the biodrying technology, the aim of this work was to study the SS biodrying process performance and, specially, to acquire knowledge about the GHGs and odorant gaseous emission patterns related to this treatment. Emission factors for specific pollutants are provided, as well as a screening on the diversity of VOC families found in the gaseous emissions from the biodrying of SS, which can be valuable information in further environmental assessment studies.

2. Materials and methods

2.1. Characteristics of feedstock

SS was obtained from the wastewater treatment plant of Navàs, Barcelona, which treats 1500 $m^3 \cdot d^{-1}$ of domestic wastewater. Diatomaceous earth (DE), which was used as a high-energy content co-substrate to enhance metabolic activity and to adjust moisture content (Johnson, 1997), was obtained from the organic fraction of Municipal Solid Waste (MSW) biomethanization plant of Can Barba in Terrassa, Barcelona. Finally, pruning waste (PW), used as bulking agent, was obtained from the composting plant of Manresa, Barcelona. The mixture was prepared manually with an industrial mixer, and the used mixing ratio of the three feedstocks (SS:DE:PW) was 1:0.25:3 on a volume basis and 1:0.15:0.48 on weight basis, which is a typical mixing ratio used during SS composting (González et al., 2019a; Maulini-Duran et al., 2013). As

aforementioned, the addition of a 10-15% of DE (weight basis) has been reported to enhance the metabolic activity of the mixture in different treatment processes (Pognani et al., 2012). Table 1 shows the physical-chemical characteristics of each material and mixture.

2.2. Experimental set-up and process operation

Figure 1 shows a scheme of the biodrying pilot plant. A cylindrical bioreactor with an operative volume of 100 L was used to carry out the SS biodrying process. The reactor was filled with 41.4 kg of the mixture with a density of 414 $kg \cdot m^{-3}$. The dimensions of reactor were 0.85 m high and had a diameter of 0.50 m. The internal and external walls of the reactor were made of stainless steel. A thermal isolation layer of polyurethane foam (2 cm) was used to avoid heat losses and to maintain near-to-adiabatic conditions. A perforated plate was fixed at the bottom of the reactor to support the material and to facilitate aeration, working as a diffusor. The biodrying reactor was opened but covered with a straw cover to prevent heat loss and vapour condensation on the mixture. Temperature of the material was measured with a temperature probe (PT-100, Iserntech S.A., Spain) introduced into the reactor, with sensors located at the top, middle and bottom of each one. An air compressor (Dixair DNX 2050, Worthington Creyssensac, Spain) and digital mass flow controllers (D-6311-DR, Bronkhorst High-Tech B. V., Ruurlo, Netherlands) were used for continuous aeration. During biodrying, the aeration flowrate was regulated based on the temperature of the material using a feedback control loop. The control software adapted the aeration level depending on different temperature ranges referred to the temperature in the middle of the reactor (<35 ºC; 35-45 ºC; 45-55 ºC; 55-70 ºC; >70 ºC), increasing the airflow rate when the material temperature increased (2, 6, 10, 14 and 20 $L \cdot min^{-1}$, corresponding to 0.12, 0.36, 0.60, 0.84 and 1.20 $L \cdot min^{-1} \cdot kg^{-1}$ of initial total VS of mixture). In this case, the middle

temperature was used to regulate airflow because both the bottom and the top temperatures of the reactor can be influenced by the temperature of the inlet airflow or due to the loss of volume of the material along the biodrying process, respectively. To follow the evolution of the process in terms of biodegradation, the oxygen content of the outlet gas of the reactor was monitored using an O_2 sensor (O2 A1, Alphasense, UK) located after a condensation trap to prevent sensors damage. The biodrying process lasted 13 days and the material was mixed manually every day during the thermophilic phase and every two days during the mesophilic stage. Water and VS loss during the biodrying process was monitored through weight loss using a scale (Gram Precision k3-k3i, Gram Group, Spain). Arduino UNO was used for data acquisition and LabView 2017® was used for data analysis and airflow control.

2.3. Gas sampling and analysis methodologies

A semi-spherical stainless steel flux chamber (0.443 m of base diameter, 0.154 m^2 of base area and 0.045 m^3 of volume) provided by Scentroid (IDES Canada Inc., Whitchurch-Stouffville, ON, Canada) was used daily to perform emissions sampling (González et al., 2019b). Nalophan® bags were used to store gas samples, which were flushed twice before obtaining the final gaseous sample for analysis. All gas samples were always obtained before mixing of the material.

CH_4 and N_2O analysis were performed using an Agilent 6890N Gas Chromatograph (GC) (Agilent Technologies, Inc., Santa Clara, CA, USA), equipped with a flame ionization detector (FID) and an electron capture detector (ECD) for CH_4 and N_2O detection, respectively. The column used for the analysis was a HP-PLOT Q semi-capillary column (30 m x 0.53 mm x 40.0 µm, Agilent Technologies, Inc.) with N_2 as carrier gas at 2 psi pressure, and a post-column particle trap (2 m, nº 5181-3352, Agilent Technologies, Inc.). For CH_4 analysis, the injector temperature was 240 ºC, the detector

163 temperature was 250 ºC and the oven, which worked isothermally, was set at 60 ºC. For
164 N_2O analysis, the injector temperature was 120 ºC, the detector temperature was 345 ºC
165 and the oven, which worked isothermally, was set at 60 ºC. The injection volume used
166 for each sample was 500 µL and the total time of analysis was 4 and 6 minutes for CH_4
167 and N_2O, respectively.

168 Odour concentration analysis were performed using a SM-100 portable field
169 olfactometer provided by Scentroid (IDES Canada, Inc., Whitchurch-Stouffville, ON,
170 Canada), as explained in González et al. (2019b). All gaseous samples were analysed
171 three times by the same panellist in a closed, well-ventilated room the same day of
172 sampling. Total volatile organic compounds (tVOCs), NH_3 and H_2S concentration of the
173 outlet gases of the reactor were measured daily in situ with a MultiRAE Lite portable
174 analyser (RAE Systems, San José, CA, USA), equipped with a 10.6 eV PID lamp for
175 tVOCs measurement and two electrochemical sensors for NH_3 and H_2S measurement,
176 respectively. tVOCs detection ranged from 0 to 1000 ppm_{veq} isobutylene with 1 ppm_{veq}
177 isobutylene increments, NH_3 detection ranged from 0 to 100 ppm_v with 1 ppm_v
178 increments and H_2S detection ranged from 0 to 100 ppm_v with 1 ppm_v increments.
179 During each analysis, the portable analyser was placed inside a closed recipient with
180 inlet and outlet ports and the outlet gases of the reactor were passed through it until a
181 steady value was read on the analyser. Since the biodrying process was held in an open
182 reactor, a suction pump was used to redirect part of the outlet gases from the surface of
183 the material to the hermetic recipient where the portable analyser was placed. The gases
184 were measured just before the water trap installed to protect the rest of the measurement
185 devices from the gaseous flow moisture.

186 To perform the VOCs characterization, two different gaseous samples of 1 L each
187 were pumped through sorbent tubes packed with two different hydrophobic sorbents

188 (Tenax® TA and Carbograph™ 1TD, Markes International, Inc., Gold River, CA,
189 USA) by means of a manual sampling pump (Markes International, Inc.). The gaseous
190 samples were obtained the 3rd and the 12th day of running, coincident with the
191 thermophilic and the mesophilic phases of the biodrying process. First, a UNITY-2
192 Thermal Desorber (TD) (Markes International, Inc.) was used to desorb the gaseous
193 samples retained in the sorbent tubes. Then, an Agilent 7820 GC coupled to an Agilent
194 5975 Mass Spectrometer (MS) (Agilent Technologies, Inc.) was used to analyse and
195 characterize the different VOCs present in the gas samples (González et al., 2019b).
196 Both samples were analysed the same day that they were obtained in order to preserve
197 the stability of VOCs in sorbent tubes (Ribes et al., 2007).

198 2.4. Estimation of the gaseous emission factors

199 The emission factor was calculated based on the measured concentration of a specific
200 pollutant, the aeration flow through the reactor at time of each sampling event and
201 normalised by the initial mass of dry matter in the SS (DM_0-SS) introduced in the
202 reactor. Firstly, daily emission rates of each pollutant were calculated (Eq. 1).

203 $$ER_i = C_i \cdot F \qquad \text{Eq. (1)}$$

204 where ER_i is the emission rate of the target pollutant (mg pollutant$\cdot d^{-1}$); C_i is the
205 concentration of the target pollutant (mg pollutant$\cdot m^{-3}$); F is the aeration flow through
206 the reactor during sampling ($m^3 \cdot d^{-1}$).

207 Then, the emission rates of a target pollutant obtained for each sampling day were
208 represented versus process time, thus the area below the curve obtained corresponds to
209 the emitted total mass of the pollutant throughout the process studied. Finally, the
210 emitted total mass of a target pollutant was divided by the initial mass of DM_0-SS
211 introduced in the reactor to obtain the emission factor (Eq. 2).

212 $$EF_i = \frac{m_i}{I}$$ Eq. (2)

213 where EF_i is the emission factor of the target pollutant (mg pollutant·kg^{-1} DM_0-SS);
214 m_i is the total emitted mass of the target pollutant during the process (mg pollutant); I is
215 the initial mass of DM_0-SS treated as specific activity index (kg DM_0-SS).

216 2.5. Analytical methods for solid samples

217 Moisture content, dry matter, organic matter content, N-Kjeldhal, C/N ratio, pH and
218 electrical conductivity were determined according to the standard procedures (US Dept.
219 of Agriculture and US Composting Council, 2001; Water Environment Federation,
220 1995). To evaluate the final biological stability of the treated material, the Dynamic
221 Respiration Index in the 24 hours of maximum biological activity (DRI_{24h}) and the
222 cumulative oxygen consumption in 4 days (AT_4) were used. These indices provide
223 information about the biological stability of an organic solid sample, and are expressed
224 in g O_2·h^{-1}·kg^{-1} VS and g O_2·kg^{-1} VS, respectively. The determination of the DRI_{24h} and
225 the AT_4 was performed using a dynamic respirometer (Ponsá et al., 2010) as explained
226 in González et al. (2019a).

227 The determination of the Higher Calorific Value (HCV) was done by means of a
228 bomb calorimeter (1341 Plain Jacket Calorimeter – 1108 Oxygen Combustion Vessel,
229 Parr, IL, USA), according to manufacturer's instructions and following the
230 methodology proposed at the DIN 51900-3:2005 (German Institute for Standarisation,
231 2003). The Lower Calorific Value (LCV) was calculated from HCV according to Eq. 3,
232 taking into account the moisture content of the final product and its estimated hydrogen
233 content (Koppejan and van Loo, 2008).

234 $$LCV = HCV \cdot \left(1 - \frac{MC}{100}\right) - \left(2.444 \cdot \frac{MC}{100}\right) - 2.444 \cdot \frac{H}{100} \cdot 8.936 \cdot \left(1 - \frac{MC}{100}\right)$$ Eq. (3)

where LCV is the Lower Calorific Value of the biomass fuel (MJ·kg^{-1} product); HCV is the Higher Calorific Value of the biomass fuel (MJ·kg^{-1} DM); MC is the moisture content of the biomass fuel (%); H is the estimated hydrogen content of the biomass fuel (%), which was considered to be a 5 % (Choi et al., 2014); 2.444 is the enthalpy difference between liquid water at 25 ºC and gaseous phase; 8.936 is the molecular weight ratio between both molecules ($mH_2O \cdot m^{-1}H_2$).

3. Results and discussion

3.1. Biodrying performance

Figure 2a shows the performance of the biodrying reactor while a summary of the process parameters evaluated during the treatment is presented in Table 2. In Figure 2a, the evolution of the temperature in the middle of the solid matrix, the specific airflow, the decrease of moisture content and the mixing pattern are represented for the whole process time. As expected, two temperature stages were encountered, a thermophilic stage (> 41 ºC) and a mesophilic stage (≤ 41 ºC). Temperature increased rapidly during the first 48 hours to the maximum values registered (51.0 ºC).

The key parameters to explain the biodrying process are temperature, specific airflow and moisture content of the solid material, which are shown in Figure 2a for the whole process time. Similar to a typical SS composting process, material temperature reached its peak on day 2. Then, temperature was maintained around 40 ºC until day 7. Thereafter, the temperature progressively decreased to a final value of 30 ºC, as previously observed in this kind of biological treatment (Huiliñir and Villegas, 2015). Specific airflow, referred to the total VS in the initial mixture (VS_0) or to the initial VS in the SS (VS_{SS}), depended on the temperature in the middle of the biodrying reactor. Its average value during the whole process was 0.46 L·min^{-1}·kg^{-1} VS_0 (2.54 L·min^{-1}·kg^{-1}

VS_{SS}), which is a typical specific airflow for SS biodrying (Cai et al., 2013; Huiliñir and Villegas, 2015) and higher than the specific airflows reported during conventional SS composting (Maulini-Duran et al., 2013; Yuan et al., 2016). These high aeration rates used in biodrying are necessary to supply oxygen to microorganisms but also to enhance water evaporation. The maximum specific airflow registered during the biodrying process (0.84 $L \cdot min^{-1} \cdot kg^{-1}$ VS_0; 4.63 $L \cdot min^{-1} \cdot kg^{-1}$ VS_{SS}), coincides with the peak of temperature found in order to maximise water evaporation during the period of maximum biological activity. In contrast, the minimum specific airflow registered (0.12 $L \cdot min^{-1} \cdot kg^{-1}$ VS_0; 0.66 $L \cdot min^{-1} \cdot kg^{-1}$ VS_{SS}) was found during the first day of biodrying, which helped to rapidly reach thermophilic conditions inside the reactor. The biodrying process was stopped on day 13, when a 34.3% reduction of the moisture content of the material was achieved, obtaining a final material with a 35.9% of moisture content, even lower to what is reported in other studies (Cai et al., 2013; Hao et al., 2018). The biodrying process time used is between typical reported values (Huiliñir and Villegas, 2015; Tambone et al., 2011) and, even though moisture content could have been reduced even more, its extension will imply higher aeration costs, especially at full-scale. The final DRI_{24h} of the biodried material was 3.5 ± 0.1 g $O_2 \cdot h^{-1} \cdot kg^{-1}$ VS, corresponding to a 44.4% reduction of the initial DRI_{24h}. Despite the DRI_{24h} reduction achieved, it is worth mentioning that the main goal of SS biodrying is not to stabilize the organic waste, but to reduce its moisture content in a short-term process to obtain a product with a LCV enough to be used as a biomass fuel. Moreover, no related literature presenting the biological stability of the final biodried material has been found for SS biodrying processes, as it happens with other wastes such as MSW (Evangelou et al., 2016). In contrast, conventional SS composting seeks reducing the biological activity of the material but applying longer process times, obtaining final $DRIs_{24h}$ lower than 1 g

284 $O_2 \cdot h^{-1} \cdot kg^{-1}$ VS (Maulini-Duran et al., 2013). Finally, the LCV of the final material was
285 analysed and was found to be 7.1 $MJ \cdot kg^{-1}$ product –increasing a 65.1% compared to the
286 initial LCV–, which is known to be sufficient for self-sustaining combustion (Hao et al.,
287 2018).

288 3.2. Greenhouse gases emissions

289 GHGs emissions from SS composting processes have been widely reported in the
290 past years due to their potential impact to global warming (Pan et al., 2018; Yuan et al.,
291 2016). However, an information gap exists about GHGs emission generated during the
292 biodrying of SS. It has to be mentioned that during this study, only GHGs emissions
293 referred to the biological process have been accounted, and CO_2 has not been taken into
294 account due to its biogenic origin. Figure 2b shows the daily emission rates of CH_4 and
295 N_2O from the biodrying processes, altogether with the temperature profile of the
296 material and the specific airflow supplied to the reactor. At first sight, two different
297 emission patterns were found for CH_4 and N_2O. In general, the CH_4 emission pattern
298 followed the temperature profile of the material, presenting its emission peak when
299 maximum temperature and maximum aeration occurred. On the other hand, N_2O
300 showed a high emission peak the first sampling day due to the stripping effect of the
301 remaining N_2O present in the SS, which rapidly decrease to lower values. However, an
302 increase of the N_2O emission was observed when the temperature of the material was
303 below 40 ^oC, suggesting that an increase in the SS biodrying process time would have a
304 negative effect in terms of GHG emissions.

305 Generally, CH_4 is formed by methanogens under anaerobic conditions. Anaerobic
306 spots can be created around the reactor by the oxygen demand at this temperature range
307 due to the rapid degradation of organic matter during thermophilic phase (Yuan et al.,
308 2016). As observed in Figure 2b, the peak of CH_4 emission coincided with that of

309 temperature, and then CH_4 emission decreased as temperature decreased into the
310 mesophilic range. Maximum and minimum CH_4 concentration measured during the SS
311 biodrying process were 8.16 ppm_v and 1.07 ppm_v, respectively.

312 The formation of N_2O is complex, which can be produced by denitrification when
313 NO_3^- is converted to N_2O and nitrogen gas, and by incomplete nitrification during the
314 conversion of NH_3 to NO_2^- (Moënne-Loccoz and Fee, 2010). The N_2O emission rates
315 for the SS biodrying process are presented in Figure 2b. During the first sampling day, a
316 peak of N_2O emission appeared, mainly because of the stripping effect of remaining
317 N_2O present in the SS used for the experiment. Once this first N_2O was stripped out of
318 the SS, there was no sign of N_2O production until the temperature of the material
319 decreased to a mesophilic range. At that point, an increase of the N_2O emission
320 appeared until the end of the process. Results suggest that the temperature of the
321 material below the high-end of the mesophilic range (40ºC), together with the low
322 carbon availability at the latter stages of the process, affected the microbial activity and,
323 concomitantly, the formation and stripping of N_2O. Under these conditions some
324 denitrifying bacteria can promote the N_2O formation by NO_3^- denitrification at the end
325 of the process (Ahn et al., 2011; Fukumoto et al., 2003). This fact should be confirmed
326 by characterizing the activity and the diversity of the bacterial communities in future
327 works. Moreover, and despite the forced aeration and the fact that the material was
328 mixed every day, different anoxic spots could had been formed inside the reactor and
329 promote the formation of N_2O by denitrification (Awasthi et al., 2018). Maximum and
330 minimum N_2O concentrations measured during the SS biodrying process were 18.75
331 ppm_v and 0.37 ppm_v, respectively.

332 Table 3 shows the emission factor of each GHG in the SS biodrying process as kg of
333 CH_4 or N_2O per Mg DM_0-SS and per Mg DM_0 of mixture and in kg of CO_{2eq} per Mg

DM_0-SS and per Mg DM_0 of mixture, respectively. These emission factors are valuable information to help comparing different treatment strategies and evaluating its environmental impact. Besides, it is important to highlight the much higher environmental impact in terms of Global Warming Potential of N_2O (265 times higher than that of CO_2) compared with CH_4 (28 times higher than that of CO_2) (IPCC, 2014). To contextualize the results obtained, the GHG emission factors have been contrasted with GHG emission factors obtained from SS composting, because, to the authors' knowledge, no previous GHG emission factors from SS biodrying have been reported. For example, Yuan et al. (2016) reported GHG emission factors depending on the aeration rate in the range of 170.43 – 272.52 kg $CO_{2eq}{\cdot}Mg^{-1}$ DM_0-SS during the composting of dewatered non-digested sewage sludge with cornstalks as bulking agent in a 60 L aerated bench-scale reactor. On the other hand, Maulini-Duran et al. (2013) found lower GHG emission factors referred to the SS composting in a 50 L aerated bench-scale reactor, using wood chips as bulking agent, ranging from 4.98 to 9.90 kg $CO_{2eq}{\cdot}Mg^{-1}$ DM_0-SS. Pan et al. (2018) observed GHG emission factors ranging from 36.05 to 134.56 kg $CO_{2eq}{\cdot}Mg^{-1}$ DM_0 of mixture while composting dewatered SS with wheat straw and different acidic additives in a 150 L bench-scale composting reactor. Moreover, the GHG emission factor related to SS biodrying process was lower than those reported for conventional SS drying systems, which are in a higher range between 367 to 21900 kg $CO_{2eq}{\cdot}Mg^{-1}$ DM_0-SS due to the use of fossil fuels and chemicals (Chen and Kuo, 2016). In comparison with the experimental emission factors reported for SS composting processes, the SS biodrying treatment seems a feasible technology in terms of GHG emission impact. However, future studies are warranted to minimise N_2O emissions by understanding the biological pathways for N_2O generation during the SS degradation and the effect of the aeration rate on its emission in order to decrease the

359 total GHGs emissions related to the SS biodrying process. Ensuring aerobic conditions
360 in the SS biodrying reactor is a key factor to minimize GHG emissions. As reported by
361 different authors studying SS composting processes, low aeration and inadequate initial
362 moisture content have a great impact on increasing GHG emission (Villegas and
363 Huiliñir, 2014; Yuan et al., 2016). Results reported herein are a good starting point for
364 future environmental impact assessment of the SS biodrying technology, which can be
365 used for Life Cycle Assessment studies.

366 3.3. Odorant compounds emissions

367 3.3.1. NH_3, H_2S, tVOCs and odour emissions

368 Emissions of NH_3, H_2S, tVOCs and odour from the SS biodrying process were
369 monitored during the whole process to fill the existing knowledge gap about gaseous
370 emissions associated to this SS biological treatment. Table 3 presents the emission
371 factors obtained as kg of pollutant per Mg DM_0-SS and per Mg DM_0 of mixture,
372 respectively, and in ou per Mg DM_0-SS and per Mg DM_0 of mixture, respectively, when
373 monitoring the biodrying processes. NH_3, H_2S, tVOCs are the typical precursors of
374 odour nuisance generated during the biological treatment of organic wastes such as SS.
375 NH_3 emissions during aerobic biodegradation of organic wastes have been widely
376 reported (Colón et al., 2012; He et al., 2017), and it is known to occur at their maximum
377 rate during the thermophilic phase of the biological process, since high temperatures
378 favour NH_3 volatilization by displacing the NH_4^+/NH_3 equilibrium to NH_3. H_2S during
379 SS biological treatment also occurs during the first stage of the process and it is
380 enhanced by high temperatures. Its formation results from bacterial reduction of
381 sulphate and decomposition of sulphur-containing compounds present in the SS under
382 anaerobic conditions (Chen et al., 2010). VOCs have been also reported to be released
383 at their highest production rate during the initial forced aeration of the biological

384 treatment of SS. In this case, NH_3, H_2S and tVOCs maximum concentrations measured
385 during SS biodrying were 330 ppm_v of NH_3, 1 ppm_v of H_2S and 18 ppm_{veq} isobutylene,
386 respectively, which were all observed during the peak of maximum temperature of the
387 material in the reactor. In SS composting processes, different ranges of target pollutants
388 concentration can be found in literature depending on the characteristics of the
389 feedstocks or the composting process itself. Hort et al. (2009) reported NH_3
390 concentrations above 70 ppm_v during the bench-scale SS and yard waste composting,
391 but no H_2S was reported due to a proper aeration of the material during the first steps of
392 the biological process. Besides, Pagans et al. (2006) reported maximum concentrations
393 of 132 ppm_v of NH_3 and 260 ppm_v of C-tVOCs while composting raw sludge in a
394 forced-aerated 30 L lab-scale reactor. On the other hand, González et al. (2019a)
395 measured NH_3 and tVOCs of 250 ppm_v and 18 ppm_v, respectively, during the SS
396 composting in a full-scale composting plant.

397 To put the obtained results into context, the emission factors of the SS biodrying
398 process have been compared with other reported emission factors from different
399 composting processes, since no information has been found about other biodrying
400 processes. Maulini-Duran et al. (2013) reported NH_3 and tVOCs emission factors in the
401 range of 1.33 to 4.12 kg $NH_3 \cdot Mg^{-1}$ DM_0-SS and 0.66 to 1.00 kg C-VOC$\cdot Mg^{-1}$ DM_0-SS,
402 respectively, during composting of raw sludge in a 50 L aerated bench-scale reactor.
403 Rincón et al. (2019) studied the gaseous emissions from the SS composting in a 300 L
404 pilot-scale reactor, reporting an NH_3 emission factor of 2.16 kg $NH_3 \cdot Mg^{-1}$ DM_0 of SS
405 and a tVOCs emission factor of 1.21 kg C-VOC$\cdot Mg^{-1}$ DM_0-SS. González et al. (2019a)
406 studied the emission of NH_3 and tVOCs in a full-scale sewage sludge composting plant,
407 reporting emission factors of 8.53 kg $NH_3 \cdot Mg^{-1}$ DM_0 of mixture and 2.09 kg C-
408 VOC$\cdot Mg^{-1}$ DM_0 of mixture. In addition, Gomez-Rico et al. (2008) and Deviatkin et al.

(2019) reported higher tVOCs and NH_3 emission factors (0.59 kg C-VOC·Mg^{-1} DM_0-SS and 1.03 to 6.00 kg NH_3·Mg^{-1} DM_0-SS, respectively) during different conventional drying of SS at 100-120ºC at lab-scale. The variability between the different studies shows that, even by treating the same type of organic waste, the substrates nature and process conditions (aeration level, initial moisture, scale, etc.) affect the emission of the odorant pollutants. However, results obtained in the present work represent a valuable insight that will allow a better understanding of the environmental impact related to this new technology.

Figure 2c shows the daily odour emission rates (OER) obtained during the SS biodrying process. Similarly to other works where odour emission from SS composting were studied (González et al., 2019b; Rincón et al., 2019) the odour emission profile reached its maximum during the thermophilic phase, when biological activity was higher. Temperature is one of the key factors affecting the emission of odorant compounds during SS biodrying. However, reaching thermophilic conditions during the process, as well as in SS composting, is inevitable and needed to obtain a proper drying of the material. Maximum odour concentration measured during SS biodrying was 3043 ou·m^{-3}. As the process proceeded, odour emissions decreased progressively down to low odour concentrations between 275 and 290 ou·m^{-3}. In this sense, few works dealing with the OEFs of SS biological treatment have been found. Rincón et al. (2019) evaluated the OEFs of different substrates in a 300 L aerated pilot-scale reactor, reporting an OEF of 9.35E+08 ou·Mg^{-1} DM_0-SS and González et al. (2019b) obtained an OEF of 9.45E+07 ou·Mg^{-1} DM_0-SS in a full-scale sewage sludge composting plant. Nevertheless, some works have been conducted over different treatment facilities to estimate their OEFs. Sironi et al. (2006) and Zarra et al. (2016) reported OEFs of 1.01E+08 ou·Mg^{-1} of MSW and 4.15E+06 ou·Mg^{-1} of MSW, respectively, from

434 different MSW mechanical-biological treatment plants. The obtained results in terms of
435 DM_0 of biodryied mixture show that OEF referred to the SS biodrying process are
436 between one and two orders of magnitude below the OEFs found in the few literature
437 mentioned, what represents lower odour impact from this kind of technology. Even
438 though these results are valuable information that can help to estimate odour emissions
439 from this biological process and the odour impact derived from similar process, they
440 must be carefully used when extrapolating into larger SS biodrying treatment systems
441 due to its dependence on different aspects such as feedstock characteristics, operational
442 parameters or plant capacity.

443 In summary, the main advantages that can be highlighted from SS biodrying over SS
444 composting are that SS biodrying is a faster biological treatment that requires less space
445 to treat the same flux of material, that energy recovery is produced and that lower
446 gaseous emissions are generated. However, it can be a more expensive alternative than
447 SS composting due to the high aeration requirements.

448 3.3.2. VOCs characterization

449 A chemical characterization was made by comparing the VOC families found in the
450 different samples as well as by quantifying the concentration of 17 out of the 35
451 detected compounds. Figure 3 presents the distribution of the different VOC families
452 found in the samples of two different days obtained during the SS biodrying process.
453 Terpenes –with α-pinene as predominant– are the main VOC family found in the
454 gaseous samples analysed, with relative abundances between 70-80%. Furthermore,
455 other odorant species such as sulphur compounds –dimethyl sulphide (DMS), dimethyl
456 disulphide (DMDS) and dimethyl trisulphide (DMTS)–, ketones –mainly 2-butanone
457 and 2-nonanone– and some alkanes and alkenes such as pentane or pentene appeared in
458 different percentages. Generally, terpenes such as α-pinene, β-pinene or limonene may

originate as intermediate products of aerobic biodegradation of organic matter. Besides, terpenes are also related to the PW used as bulking agent for the biodrying process (González et al., 2019b; Schiavon et al., 2017). In the present work, its abundance was that high probably due to the high SS:PW v/v ratio used. On the other hand, sulphur compounds are typical chemicals present in the gaseous emissions generated during the SS treatment, which are normally formed and emitted during the first stages of the SS biological treatment (He et al., 2017; Schiavon et al., 2017). In the work presented herein, a 13% abundance of organosulphur compounds was found in the first sample, which coincide with the thermophilic phase of the biological process. Then, when the process fell into mesophilic temperature, the organosulphur compounds abundance decreased to 3%. Finally, some other odorant compounds typically found in the gaseous emissions generated during the biological treatment of SS were found, such as ketones, alkanes or alkenes. Ketones were found at maximum abundance during the first stage of the SS biodrying (6.6% abundance), which was then reduced down to a 0.5% abundance during the mesophilic phase.

4. Conclusions

Results indicated a proper performance of the SS biodrying process. The corresponding GHG and odorant emissions were accounted to be lower than that reported for conventional SS composting. GHG emission factor and OEF referred to the bench-scale SS biodrying process were 28.22 kg CO_{2eq}·Mg^{-1} DM_0-SS and 3.10E+07 ou·Mg^{-1} DM_0-SS, respectively. In conclusion, since there is no available scientific information dealing with the gaseous emissions from SS biodrying to compare with, this study shows a new insight into the gaseous emissions generated during the SS biodrying process at bench-scale, which will serve in further development of this treatment.

E-supplementary data for this work can be found in e-version of this paper online.

References

1. Adani, F., Baido, D., Calcaterra, E., Genevini, P., 2002. The influence of biomass temperature on biostabilization-biodrying of municipal solid waste. Bioresour. Technol. 83, 173–179. doi:10.1016/S0960-8524(01)00231-0

2. Ahn, H.K., Mulbry, W., White, J.W., Kondrad, S.L., 2011. Pile mixing increases greenhouse gas emissions during composting of dairy manure. Bioresour. Technol. 102, 2904–2909.

3. Awasthi, M.K., Wang, Q., Chen, H., Wang, M., Awasthi, S.K., Ren, X., Cai, H., Li, R., Zhang, Z., 2018. In-vessel co-composting of biosolid: Focusing on mitigation of greenhouse gases emissions and nutrients conservation. Renew. Energy 129, 814–823.

4. Cai, L., Chen, T., Gao, D., Zheng, G., Liu, H., 2013. Influence of forced air volume on water evaporation during sewage sludge bio-drying. Water Res. 47, 4767–4773.

5. Capelli, L., Sironi, S., Del Rosso, R., Céntola, P., 2009. Predicting odour emissions from wastewater treatment plants by means of odour emission factors. Water Res. 43, 1977–1985.

6. Capelli, L., Sironi, S., Rosso, R. Del, 2014. Odour Emission Factors: Fundamental Tools for Air Quality Management. Chem. Eng. Trans. 40.

7. Chen, J., Liu, H.-T., Lei, M., Chen, T.-B., Zheng, G.-D., Gao, D., Guo, S.-L., Cai, L., 2010. Reducing H2S production by O2 feedback control during large-scale sewage sludge composting. Waste Manag. 31, 65–70.

8. Chen, Y.C., Kuo, J., 2016. Potential of greenhouse gas emissions from sewage sludge management: A case study of Taiwan. J. Clean. Prod. 129, 196–201.

9. Choi, H.L., Sudiarto, S.I.A., Renggaman, A., 2014. Prediction of livestock manure and mixture higher heating value based on fundamental analysis. Fuel 116, 772–780.

10. Colón, J., Cadena, E., Pognani, M., Barrena, R., Sánchez, A., Font, X., Artola, A., 2012. Determination of the energy and environmental burdens associated with the biological treatment of source-separated Municipal Solid Wastes. Energy Environ. Sci. 5, 5731–5741.

11. Cometto-Muñiz, J.E., Cain, W., Abraham, M., Kumarsingh, R., 1998. Sensory properties of selected terpenes. Thresholds for odor, nasal pungency, nasal localization, and eye irritation. Ann. N. Y. Acad. Sci. 855, 648–651.

12. Deviatkin, I., Lyu, L., Chen, S., Havukainen, J., Wang, F., Horttanainen, M., Mänttäri, M., 2019. Technical implications and global warming potential of recovering nitrogen released during continuous thermal drying of sewage sludge. Waste Manag. 90, 132–140.

13. European Commission, 2014. http://ec.europa.eu/environment/waste/sludge/ [WWW Document].

14. Evangelou, A., Gerassimidou, S., Mavrakis, N., Komilis, D., 2016. Monitoring the performances of a real scale municipal solid waste composting and a biodrying facility using respiration activity indices. Environ. Monit. Assess. 188.

15. Frei, K.M., Cameron, D., Stuart, P.R., 2004. Novel drying process using forced aeration through a porous biomass matrix. Dry. Technol. 22, 1191–1215.

16. Fukumoto, Y., Osada, T., Hanajima, D., Haga, K., 2003. Patterns and quantities of NH3, N2O and CH4 emissions during swine manure composting without forced

530 aeration - Effect of compost pile scale. Bioresour. Technol. 89, 109–114.

531 17. German Institute for Standarisation, 2003. DIN 51900-3:2005. Testing of solid and
532 liquid fuels - Determination of gross calorific value by the bomb calorimeter and
533 calculation of net calorific value - Part 3: Method using the adiabatic jacket.

534 18. Gomez-Rico, M.F., Fullana, A., Font, R., 2008. Volatile organic compounds
535 released from thermal drying of sewage sludge. WIT Trans. Ecol. Environ. 111,
536 425–433.

537 19. González, D., Colón, J., Gabriel, D., Sánchez, A., 2019a. The effect of the
538 composting time on the gaseous emissions and the compost stability in a full-scale
539 sewage sludge composting plant. Sci. Total Environ. 654, 311–323.

540 20. González, D., Colón, J., Sánchez, A., Gabriel, D., 2019b. A systematic study on the
541 VOCs characterization and odour emissions in a full-scale sewage sludge
542 composting plant. J. Hazard. Mater. 373, 733–740.

543 21. Hao, Z., Yang, B., Jahng, D., 2018. Combustion characteristics of biodried sewage
544 sludge. Waste Manag. 72, 296–305.

545 22. He, P., Wei, S., Shao, L., Lü, F., 2017. Emission potential of volatile sulfur
546 compounds (VSCs) and ammonia from sludge compost with different bio-stability
547 under various oxygen levels. Waste Manag. 73, 113–122.

548 23. Hort, C., Gracy, S., Platel, V., Moynault, L., 2009. Evaluation of sewage sludge and
549 yard waste compost as a biofilter media for the removal of ammonia and volatile
550 organic sulfur compounds (VOSCs). Chem. Eng. J. 152, 44–53.

551 24. Huiliñir, C., Villegas, M., 2015. Simultaneous effect of initial moisture content and
552 airflow rate on biodrying of sewage sludge. Water Res. 82, 118–128.

553 25. IPCC, 2014. Climate Change 2014: Synthesis Report. Contribution of Working
554 Groups I, II and III to the Fifht Assessment Report of the Intergovernmental Panel
555 on Climate Change. IPCC, Geneva, Switzerland.

556 26. Johnson, M., 1997. Management of spent diatomaceous earth from brewing
557 industry.

558 27. Kim, H., Hao, Z., Yang, B., Kim, S., Kwon, G., Jahng, D., 2018. Characterization
559 and Treatment of Emission Gas Condensate Generated from Biodrying of Sewage
560 Sludge. Environ. Eng. Sci. 35, ees.2017.0362.

561 28. Koppejan, J., van Loo, S., 2008. The Handbook of Biomass Combustion and Co-
562 firing. Earthscan, London.

563 29. Leffingwell, 2018. http://www.leffingwell.com/odorthre.htm, Accessed on
564 December 2018. [WWW Document].

565 30. Maulini-Duran, C., Artola, A., Font, X., Sánchez, A., 2013. A systematic study of
566 the gaseous emissions from biosolids composting: Raw sludge versus
567 anaerobically digested sludge. Bioresour. Technol. 147, 43–51.

568 31. Moënne-Loccoz, P., Fee, J.A., 2010. Catalyzing NO to N2O in the nitrogen cycle.
569 Science (80-.). 330, 10–11.

570 32. Nagata, Y., 2003. Odor measurement review, Measurement of odor threshold by
571 triangle odor bag method. Minist. Enviornmental Gov. Japan 122–123.

572 33. Pagans, E., Font, X., Sánchez, A., 2006. Emission of volatile organic compounds
573 from composting of different solid wastes: Abatement by biofiltration. J. Hazard.
574 Mater. 131, 179–186.

575 34. Pan, J., Cai, H., Zhang, Z., Liu, H., Li, R., Mao, H., Awasthi, M.K., Wang, Q., Zhai,

576 L., 2018. Comparative evaluation of the use of acidic additives on sewage sludge
577 composting quality improvement, nitrogen conservation, and greenhouse gas
578 reduction. Bioresour. Technol. 270, 467–475.

579 35. Pognani, M., Barrena, R., Font, X., Sánchez, A., 2012. A complete mass balance of
580 a complex combined anaerobic/aerobic municipal source-separated waste
581 treatment plant. Waste Manag. 32, 799–805.

582 36. Ponsá, S., Gea, T., Sánchez, A., 2010. Different Indices to Express Biodegradability
583 in Organic Solid Wastes. J. Environ. Qual. 39, 706–712.

584 37. Ribes, A., Carrera, G., Gallego, E., Roca, X., Berenguer, M.J., Guardino, X., 2007.
585 Development and validation of a method for air-quality and nuisance odors
586 monitoring of volatile organic compounds using multi-sorbent adsorption and gas
587 chromatography/mass spectrometry thermal desorption system. J. Chromatogr. A
588 1140, 44–55.

589 38. Rincón, C.A., De Guardia, A., Couvert, A., Le Roux, S., Soutrel, I., Daumoin, M.,
590 Benoist, J.C., 2019. Chemical and odor characterization of gas emissions released
591 during composting of solid wastes and digestates. J. Environ. Manage. 233, 39–53.

592 39. Schiavon, M., Martini, L.M., Corrà, C., Scapinello, M., Coller, G., Tosi, P.,
593 Ragazzi, M., 2017. Characterisation of volatile organic compounds (VOCs)
594 released by the composting of different waste matrices. Environ. Pollut. 231, 845–
595 853.

596 40. Shen, Y., Chen, T. Bin, Gao, D., Zheng, G., Liu, H., Yang, Q., 2012. Online
597 monitoring of volatile organic compound production and emission during sewage
598 sludge composting. Bioresour. Technol. 123, 463–470.

599 41. Sironi, S., Capelli, L., Céntola, P., Del Rosso, R., Il Grande, M., 2006. Odour
600 emission factors for the prediction of odour emissions from plants for the
601 mechanical and biological treatment of MSW. Atmos. Environ. 40, 7632–7643.

602 42. Tambone, F., Scaglia, B., Scotti, S., Adani, F., 2011. Effects of biodrying process on
603 municipal solid waste properties. Bioresour. Technol. 102, 7443–7450.

604 43. United States Environmental Protection Agency (USEPA), 1995. Compilation of air
605 pollutant emission factors, AP-42, vol. 1, 5th ed., Stationary point and area
606 sources. Research Triangle Park, NC, USA.

607 44. US Dept. of Agriculture, US Composting Council, 2001. Test methods for the
608 examination of composting and compost purpose, in: Edaphos International,
609 Houston.

610 45. Villegas, M., Huiliñir, C., 2014. Biodrying of sewage sludge: Kinetics of volatile
611 solids degradation under different initial moisture contents and air-flow rates.
612 Bioresour. Technol. 174, 33–41.

613 46. Water Environment Federation, 1995. Standard Methods for the Examination of
614 Water and Wastewater.

615 47. Wei, Y., Tong, J., Wang, Y., ChuLu, B., Yu, D., Sui, Q., Zhang, J., Chen, M., 2016.
616 Who contributes more to N2O emission during sludge bio-drying with two
617 different aeration strategies, nitrifiers or denitrifiers? Appl. Microbiol. Biotechnol.
618 101, 3393–3404.

619 48. Yuan, J., Chadwick, D., Zhang, D., Li, G., Chen, S., Luo, W., Du, L., He, S., Peng,
620 S., 2016. Effects of aeration rate on maturity and gaseous emissions during sewage
621 sludge composting. Waste Manag. 56, 403–410.

622 49. Zarra, T., Naddeo, V., Oliva, G., Belgiorno, V., 2016. Odour emissions
623 characterization for impact prediction in anaerobic-aerobic integrated treatment
624 plants of municipal solid waste. Chem. Eng. Trans. 54, 91–96.

625 50. Zhao, L., Gu, W.M., He, P.J., Shao, L.M., 2011. Biodegradation potential of bulking
626 agents used in sludge bio-drying and their contribution to bio-generated heat.
627 Water Res. 45, 2322–2330.

628

629

Legend to Figures

Figure 1. Scheme of the biodrying system and the external industrial mixer used during the experiment (TT represents the temperature measure; FC represents the mass flow controller; O_2T represents the O_2 measure).

Figure 2. (a) Performance of the biodrying process. In black dots, the evolution of the temperature of the material in the middle of the reactor (ºC); in white dots, the evolution of the moisture content of the solid mixture (%); solid line, the specific airflow introduced in the reactor ($L \cdot min^{-1} \cdot kg^{-1}$ VS_0), black arrows represent the mixing pattern. (b) CH_4 and N_2O emission rate profile during the biodrying process. In black dots, the temperature of the material in the middle of the reactor (ºC); in white squares, the inlet specific airflow rate ($L \cdot min^{-1} \cdot kg^{-1}$ VS_0); in blue squares, the evolution of the CH_4 emission rate (mg $CH_4 \cdot d^{-1}$); in green triangles, the evolution of the N_2O emission rate (mg $N_2O \cdot d^{-1}$). (c) Odour emission rate (OER) profile during the biodrying process. In black dots, the temperature of the material in the middle of the reactor (ºC); in white squares, the inlet specific airflow rate ($L \cdot min^{-1} \cdot kg^{-1}$ VS_0); in cyan squares, the evolution of the odour emission rate (OER, ou$\cdot d^{-1}$).

Figure 3. Distribution of the different VOC families found in each sample, expressed in percentage of abundance respect the whole sample, from the outlet gases of the biodrying reactor.

Tables

Table 1. Physical-chemical properties of the feedstocks and mixture used during the biodrying process.

Physicochemical properties	SS	PW	DE	Biodrying mixture
Moisture (%)	83.5 ± 0.1	18.0 ± 0.0	3.9 ± 0.0	54.6 ± 0.1
Organic matter (%)	68.9 ± 0.2	88.7 ± 0.0	35.2 ± 0.1	85.2 ± 0.0
C/N ratio	9.1	31.6	1321.6	13.6
pH	6.7	8.2	6.2	–
Electrical conductivity (mS/cm)	2.5	1.7	1.2	–
DRI_{24h} (g $O_2 \cdot h^{-1} \cdot kg^{-1}$ VS)	7.3 ± 0.9	–	–	6.3 ± 1.7

SS: sewage sludge; PW: pruning waste; DE: diatomaceous earth

653 Table 2. Summary of the process parameters evaluated during the biodrying process.

Parameter			Biodrying	Units
Air supplied	Total air volume		1.4E+05	L
	Average air supply		0.46	$L \cdot min^{-1} \cdot kg^{-1}$ VS_0
			2.54	$L \cdot min^{-1} \cdot kg^{-1}$ VS_{SS}
Total evaporated water			13.3	kg H_2O
Calorific value	HCV	Initial	15.1 ± 0.1	$MJ \cdot kg^{-1}$ TS
		Final	13.6 ± 0.2	
	LCV	Initial	4.3 ± 0.1	$MJ \cdot kg^{-1}$ product
		Final	7.1 ± 0.1	
Biological stability	DRI_{24h}	Initial	6.3 ± 1.7	g $O_2 \cdot h^{-1} \cdot kg^{-1}$ VS
		Final	3.5 ± 0.1	
	AT_4	Initial	403.6 ± 43.8	g $O_2 \cdot kg^{-1}$ VS
		Final	175.1 ± 18.9	

654 HCV: higher calorific value; LCV: Lower Calorific Value

Table 3. CH_4, N_2O, NH_3, tVOCs and odour emission factors for the biodrying process. GHG emission factors are expressed in kg of pollutant and in kg of CO_2 equivalent per Mg DM_0-SS and Mg DM_0 of mixture, respectively. Odorant emission factors are expressed in kg of pollutant per Mg DM_0-SS and Mg DM_0 of mixture and odour emission factor is expressed in ou per Mg DM_0-SS and Mg DM_0 of mixture, respectively.

		kg pollutant·Mg^{-1} DM_0-SS	kg pollutant·Mg^{-1} DM_0
GHGs	CH_4 emission factor	4.54E-02	1.02E-02
	N_2O emission factor	1.02E-01	2.28E-02
		kg CO_{2eq}·Mg^{-1} DM_0-SS	kg CO_{2eq}·Mg^{-1} DM_0
GHGs	CH_4 emission factor [a]	1.27	0.28
	N_2O emission factor [a]	26.95	6.04
	GHG emission factor [a, b]	28.22	6.32
		kg pollutant·Mg^{-1} DM_0-SS	kg pollutant·Mg^{-1} DM_0
Odorants	NH_3 emission factor	1.23	2.75E-01
	H_2S emission factor	1.68E-03	3.77E-04
	tVOCs emission factor	1.38E-01	3.10E-02
		ou·Mg^{-1} DM_0-SS	ou·Mg^{-1} DM_0
Odour	Odour emission factor	3.10E+07	6.95E+06

[a] GHGs emission for CH_4 and N_2O, on a 100-yr frame, is 28 and 265 times higher than that of CO_2, respectively (IPCC, 2014).

[b] GHGs emission factor as the sum of the CH_4 and N_2O emission factors.

Figures

FIGURE 1

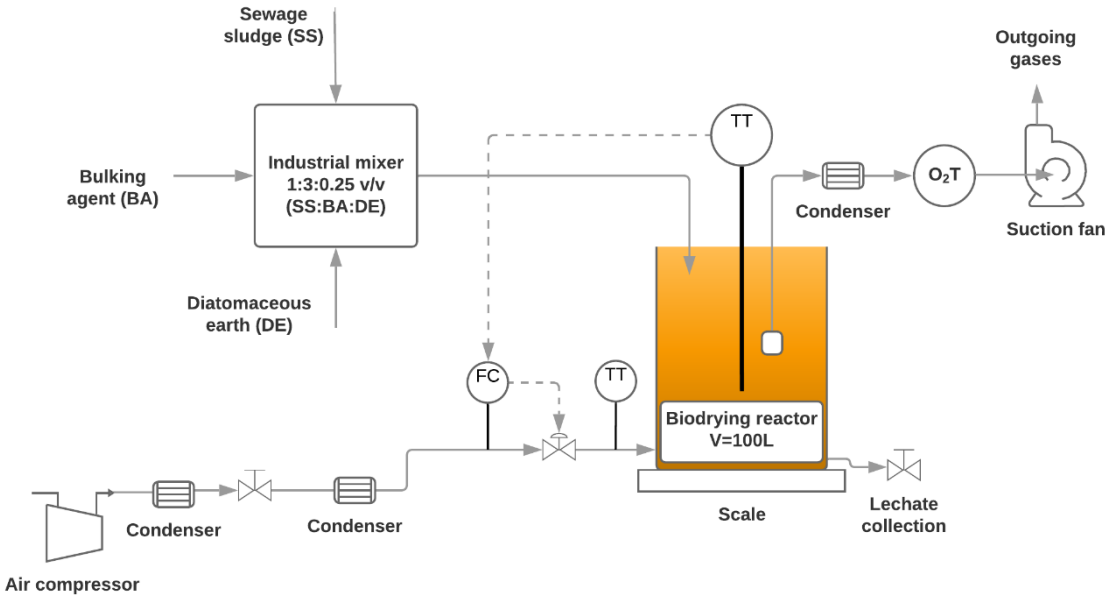

667 FIGURE 2

668 a)

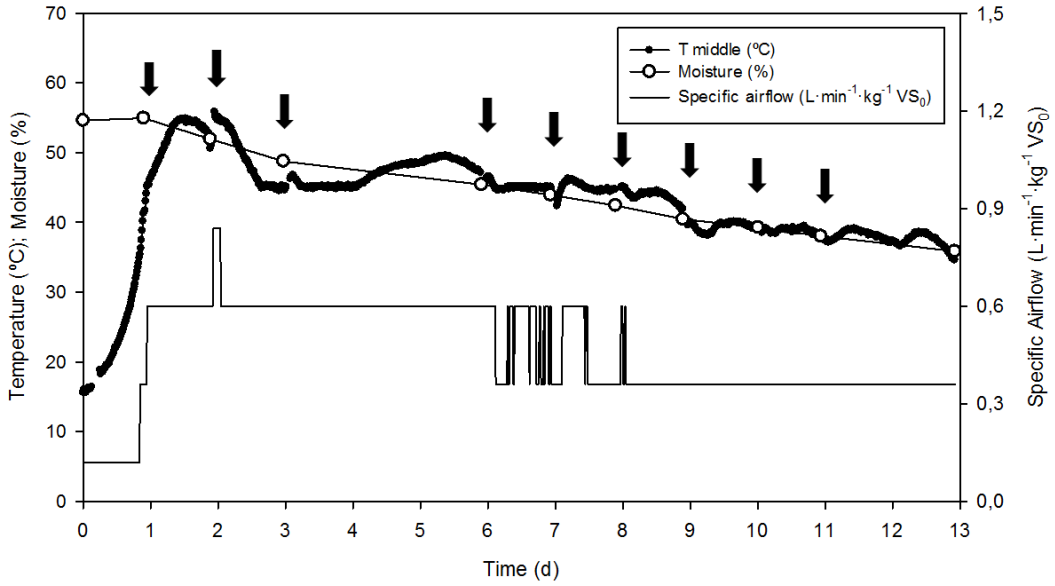

669

670 b)

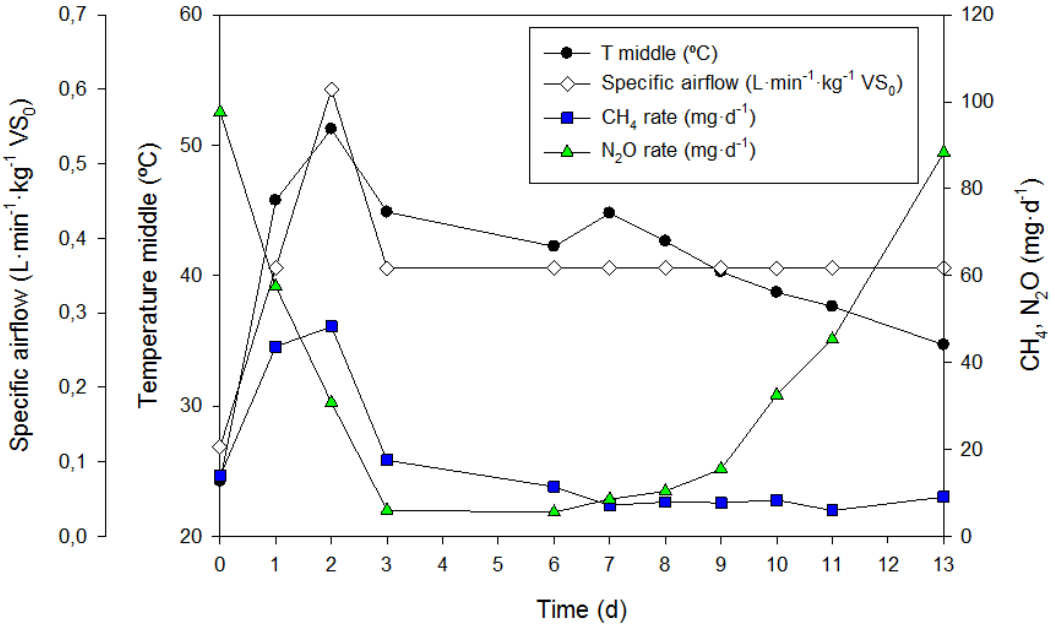

671

672

673

674 c)

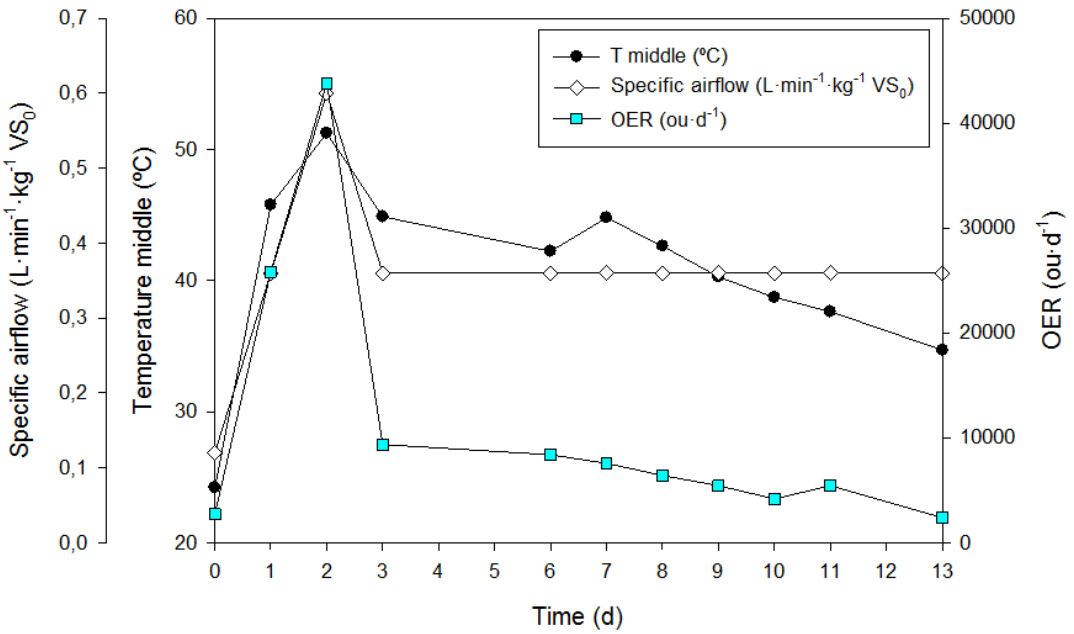
T middle (ºC)
Specific airflow (L·min-1·kg-1 VS0)
OER (ou·d-1)
Specific airflow (L·min-1·kg-1 VS0)
Temperature middle (ºC)
OER (ou·d-1)
Time (d)
0,0
0,1
0,2
0,3
0,4
0,5
0,6
0,7
20
30
40
50
60
0
10000
20000
30000
40000
50000
0
1
2
3
4
5
6
7
8
9
10
11
12
13

675

676

677 FIGURE 3

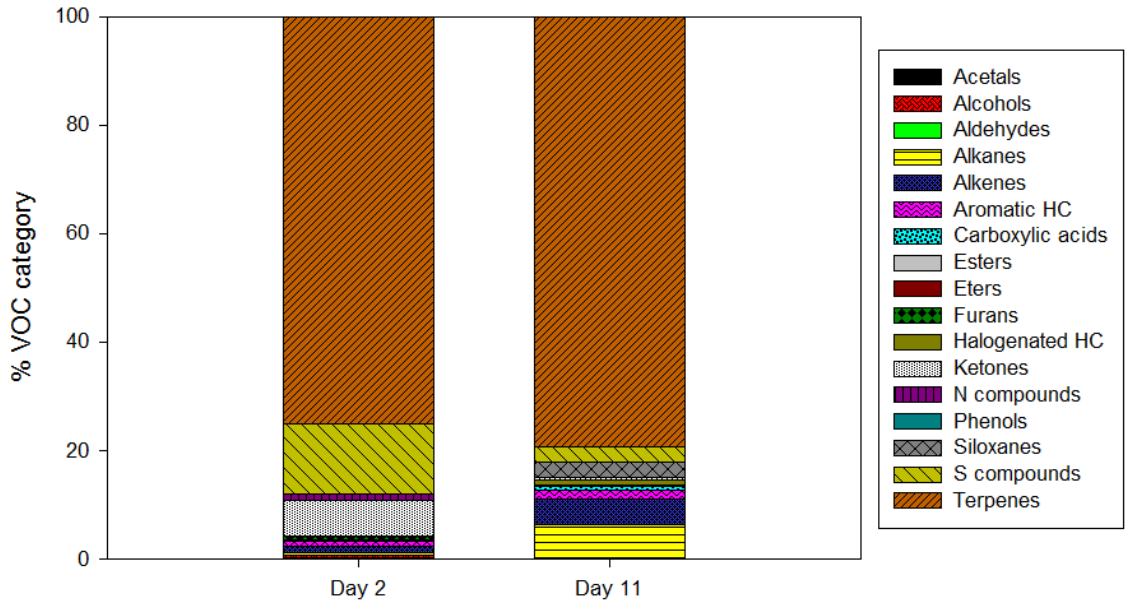

678

679

Filling in sewage sludge biodrying gaps: Greenhouse gases, volatile organic compounds and odour emissions

(E-Supplementary Information)

Daniel González [a, b], Nagore Guerra [c], Joan Colón [c], David Gabriel [b], Sergio Ponsá [c], Antoni Sánchez [a, *]

[a] *Composting Research Group (GICOM) Dept. of Chemical, Biological and Environmental Engineering, Universitat Autònoma de Barcelona, 08193-Bellaterra (Barcelona), Spain.*

[b] *Group of biological treatment of liquid and gaseous effluents (GENOCOV) Dept. of Chemical, Biological and Environmental Engineering, Universitat Autònoma de Barcelona, 08193-Bellaterra (Barcelona), Spain*

[c] *BETA Technology Centre: "U Science Tech", University of Vic-Central University of Catalonia, 08500 Vic, Barcelona, Spain*

* Corresponding author:

Antoni Sánchez

Composting Research Group (GICOM), Dept. of Chemical, Biological and Environmental Engineering

Universitat Autònoma de Barcelona

Bellaterra, 08193 (Spain)

Email address: antoni.sanchez@uab.cat

E-Supplementary Information

Table 1S. Quantified VOCs in the gaseous samples obtained from the biodrying monitoring, with its odour detection threshold (ODT), expressed in ppb_v ("<DL": compound concentration below the detection limit; "–": not detected compound).

Family	Compound	ODT (ppb_v)	Biodrying	
			Day 2	Day 11
Alcohols	1-butanol	38[a]	–	–
	1-hexanol	0.006[a]	–	–
Aldehydes	n-hexanal	4.5-5[b]	–	–
	Octanal	0.01[a]	–	–
	Decanal	0.1-2[b]	–	–
	Isovaleraldehyde	0.1[a]	42.1	–
	Benzaldehyde	350[b]	–	–
Alkanes	Hexane	1.5[a]	–	–
	Heptane	670[a]	<*DL*	–

	Decane	620[a]	–	–
Aromatic HC	Benzene	2700[a]	<*DL*	<*DL*
	Toluene	330[a]	3.9	<*DL*
	Ethylbenzene	0.17[a]	<*DL*	–
	m-xylene	0.041[a]	<*DL*	–
	Styrene	35[a]	16.9	–
Carboxylic acids	Butanoic acid	0.19[a]	–	–
Esters	Ethyl butyrate	0.00004[a]	–	–
	Ethyl valerate	0.00011[a]	–	–
Ethers	2-buthoxyethanol	0.043[a]	–	–
Halogenated HC	Tetrachloroethylene	0.77[a]	–	–
Ketones	2-butanone	440[a]	1037.9	–
	2-pentanone	28[a]	207.2	–
	Cyclohexanone	100[b]	–	–
N compounds	Pyridine	63[a]	201.5	–

	Indole	0.3[a]	–	–
	Skatole	0.006[a]	–	–
Phenols	Phenol	5.6[a]	–	–
S compounds	DMS	3[a]	–	48.5
	DMDS	2.2[a]	9545.7	36.5
Terpenes	α-pinene	18[a]	2955.5	165.9
	β-pinene	33[a]	1308.3	3.0
	Limonene	38[a]	955.3	10.6
	p-cymene	1200[c]	256.8	4.2
	Eucalyptol	12[b]	3782.9	–

705 [a] (Nagata, 2003)

706 [b] (Leffingwell, 2018)

707 [c] (Cometto-Muñiz et al., 1998)